Hindawi
Complexity
Volume 2023, Article ID 6626189, 11 pages
https://doi.org/10.1155/2023/6626189

Research Article

A Numerical Approach for the Analytical Solution of Multidimensional Wave Problems

Jinxing Liu,[1] **Jiahua Fang**,[2] **Muhammad Nadeem**,[3] **and Yahya Alsayyad**[4]

[1]*Faculty of Science, Yibin University, Yibin 644000, China*
[2]*Yibin University, Yibin 644000, China*
[3]*School of Mathematics and Statistics, Qujing Normal University, Qujing 655011, China*
[4]*Department of Physics, Hodeidah University, Al-Hudaydah, Yemen*

Correspondence should be addressed to Yahya Alsayyad; yahyaalsayyad2022@hoduniv.net.ye

Received 1 May 2023; Revised 20 October 2023; Accepted 23 December 2023; Published 31 December 2023

Academic Editor: Abdellatif Ben Makhlouf

Copyright © 2023 Jinxing Liu et al. This is an open access article distributed under the Creative Commons Attribution License, which permits unrestricted use, distribution, and reproduction in any medium, provided the original work is properly cited.

Wave problem arises in various phenomena of science and engineering. This study proposes an efficient and appropriate scheme to produce the approximate solutions of multidimensional problems arising in wave propagation. We use a new iterative strategy (NIS) to minimize the computational cost and less time than other approaches studied in the literature. Since the variational iteration method (VIM) has some assumptions and restrictions of variables during the construction of the recurrence relation, we present a Sawi integral transform for the construction of the recurrence to overcome this difficulty. The series solution for this recurrence relation is determined using the homotopy perturbation strategy (HPS) in the form of convergence that provides the precise solution after a few iterations. This NIS does not require any discretization in the findings of results and derives the algebraic equations. Some numerical models and graphical representations are illustrated to verify the performance of this scheme.

1. Introduction

Significant improvements in computational techniques have been made recently for engineering and scientific applications such as characterization of geomaterials, soil-structure interaction, elastic metamaterials, etc., as well as the simulation of seismic wave propagation. The simulation's temporal and spatial scales, constitutive laws, interface and boundary conditions, and numerical schemes must all be carefully chosen depending on the application of interest [1–3].

The study of partial differential equations (PDEs) has an important contribution in numerous branches of science and engineering such as electronics, hydrology, computational dynamics, physical chemistry, chemical engineering, optical fiber, mechanics, dynamics of substances, and the geometric optical [4–6]. Various researchers have studied the analytical schemes to obtain the approximate solution of these PDEs. Even though the computations for these methods are quite simple, some variables are premised on the hypothesis of numerous types of restrictions. Therefore, many scientists are searching for novel approaches to solve this kind of limitations. Many experts and scientists have presented several approaches to evaluate the analytical results [7–9]. In the past, a number of experts and researchers applied the homotopy perturbation technique (HPS) [10, 11] to a variety of physical issues because this method consistently reduces the complex problem to a simple solution. The solution series converges using this strategy quite quickly in the majority of instances. The authors [12, 13] implemented the idea of the homotopy perturbation method for the nonlinear oscillation problems and showed that this scheme provided the analytical results very efficiently.

The wave problem is a PDE for a scalar function that governs the wave propagation phenomena in fluid dynamics. Wazwaz employed the VIM to research linear and nonlinear difficulties [14]. The homotopy perturbation method was utilized by Ghasemi et al. [15] to calculate the

numerical solutions of the two-dimensional nonlinear differential equation. For the approximate solution of wave problems, Keskin and Oturanc [16] proposed a new approach. Ullah et al. [17] suggested a homotopy optimal approach to derive the analytic results of wave problems. Adwan et al. [18] provided the computational results of multidimensional wave problems and demonstrated the validity of the suggested method. Jleli et al. [19] utilized the HPS for the approximate results of wave problems. The authors [20] presented the finite element approach and discretized the two-dimensional wave model to obtain the analytical results. These methods contain numerous restrictions and presumptions when it comes to estimating the solution. We provide a new iterative approach for these multidimensional wave problems and tackle these limitations and restrictions in our current research.

The aim of the current study is to apply a new iterative strategy (NIS) with the combination of the Sawi integral transform and the HPS for multidimensional problems. This NIS generates an iteration series that provides approximation results near the exact results. This scheme shows a better performance and yields attractive results for the illustrated problems. This article is studied as follows: Section 2 provides the idea of Sawi integral transform with the convergence theorem. We construct a scheme of NIS for obtaining the results of multidimensional models in Section 3. Some numerical applications are considered to show the capability of NIS in Section 4, and lastly, we present the conclusion in Section 5.

2. Fundamental Concepts

In this section, we present some essential properties of Sawi transform to understand the concept of their formulation. These properties are very helpful in utilizing the numerical problems of this paper.

2.1. Sawi Transform

Definition 1. Consider ϑ be a function of $\eta \geq 0$, then Sawi transform ($\mathbb{S}\ T$) is [21, 22]

$$\mathbb{S}[\vartheta(\eta)] = Q(\theta) = \frac{1}{\theta^2}\int_0^{\infty} \vartheta(\eta) e^{-\eta/\theta} \mathrm{dt}, \quad \eta \geq 0, k_1 \leq \theta \leq k_2, \tag{1}$$

where $\mathbb{S}$ is denoted as a symbol of $\mathbb{S}\ T$. Then, we have

$$\begin{aligned} &\mathbb{S}^{-1}[Q(\theta)] = \vartheta(\eta), \\ &\mathbb{S}^{-1} \text{ is the inverse } \mathbb{S}\mathrm{T}, \end{aligned} \tag{2}$$

where $Q(\theta)$ represents the transform function of $\vartheta(\eta)$. The Sawi transform of the function $\vartheta(\eta)$ for $\eta \geq 0$ exist if $\vartheta(\eta)$ is piecewise continuous and of exponential order. The mentioned two conditions are the only sufficient conditions for the existence of Sawi transforms of the function $\vartheta(\eta)$.

Proposition 2. *We define the fundamental properties of $\mathbb{S}\ T$ such as let $\mathbb{S}\{\vartheta_1(\eta)\} = Q_1(\theta)$ and $\mathbb{S}\{\vartheta_2(\eta)\} = Q_2(\theta)$, then [23, 24]*

$$\begin{aligned} &\mathbb{S}\{a\vartheta_1(\eta) + b\vartheta_2(\eta)\} = a\mathbb{S}\{\vartheta_1(\eta)\} + b\mathbb{S}\{\vartheta_2(\eta)\}, \\ \Longrightarrow \quad &\mathbb{S}\{a\vartheta_1(\eta) + b\vartheta_2(\eta)\} = \mathrm{aQ}_1(\theta) + \mathrm{bQ}_2(\theta). \end{aligned} \tag{3}$$

Proposition 3. *Let us define the differential properties of $\mathbb{S}\ T$ such as if $\mathbb{S}\{\vartheta(\eta)\} = Q(\theta)$, the differential properties are defined as [25]*

$$\begin{aligned} &\mathbb{S}\left\{\vartheta'(\eta)\right\} = \frac{Q(\theta)}{\theta} - \frac{\vartheta(0)}{\theta^2}, \\ &\mathbb{S}\left\{\vartheta''(\eta)\right\} = \frac{Q(\theta)}{\theta^2} - \frac{\vartheta(0)}{\theta^3} - \frac{\vartheta'(0)}{\theta^2}, \\ &\mathbb{S}\{\vartheta^m(\eta)\} = \frac{Q(\theta)}{\theta^m} - \frac{\vartheta(0)}{\theta^{m+1}} - \frac{\vartheta'(0)}{\theta^m} - \cdots - \frac{\vartheta^{m-1}(0)}{\theta^2}. \end{aligned} \tag{4}$$

Theorem 4. *Assume that φ and χ be two Banach spaces such that I: $\varphi \longrightarrow \chi$ is a nonlinear operator. Therefore, $\Psi; \Psi^* \in ; \varphi, \|I(\Psi) - I(\Psi^*)\| \leq K\|\Psi - \Psi^*\|, 0 < K < 1$. The Banach contraction states that I is denoted as a unique fixed point Ψ, i.e., $I\Psi = \Psi$, so we have*

$$\Psi(\varphi, \varsigma) = \lim_{N \longrightarrow \infty} \sum_{n=0}^{N} \Psi_n(\varphi, \varsigma), \tag{5}$$

and assume that $\varphi_0 = \Psi_0 \in \mathcal{S}_p(\Psi)$, where $\mathcal{S}_p(\Psi) = \{\Psi^* \in \varphi: \|\Psi - \Psi^*\| < p\}$ then, we have

$$\begin{aligned} &(B_1)\ \varphi_n \in \mathcal{S}_p(\Psi), \\ &(B_2)\ \lim_{n \longrightarrow \infty} \varphi_n = \Psi. \end{aligned} \tag{6}$$

Proof. (B_1) In the light of mathematical induction at $n = 1$, we have

$$\left\|\varphi_1 - \Psi_1\right\| = \left\|T(\varphi_0 - T(\Psi))\right\| \leq K\left\|\Psi_0 - \Psi\right\|. \tag{7}$$

Let the result be accurate for $n = 1$, thus

$$\left\|\varphi_{n-1} - \Psi\right\| \leq K^{n-1}\left\|\Psi_0 - \Psi\right\|. \tag{8}$$

Therefore,

$$\left\|\varphi_n - \Psi\right\| = \left\|T(\varphi_{n-1} - T(\Psi))\right\| \leq K\left\|\varphi_{n-1} - \Psi\right\| \leq K^n\left\|\Psi_0 - \Psi\right\|. \tag{9}$$

Hence, using (B_1), we have

$$\left\|\varphi_n - \Psi\right\| \leq K^n\left\|\Psi_0 - \Psi\right\| \leq K^n p < p, \tag{10}$$

which shows $\varphi_n \in \mathcal{S}_p(\Psi)$.

B_2: Since $\|\varphi_n - \Psi\| \leq K^n\|\Psi_0 - \Psi\|$ and as a $\lim_{n \longrightarrow \infty} K^n = 0$.

Therefore, we have $\lim_{n \longrightarrow \infty}\|\Psi_n - \Psi\| = 0 \Rightarrow \lim_{n \longrightarrow \infty} \Psi_n = \Psi$. □

3. Formulation of NIS

In this section, we consider 1D, 2D, and 3D wave problems for the use of the new iterative strategy (NIS). This scheme is applicable to solve the differential problems using the initial conditions. We made a point where the development of this method is independent from integration and any other presumptions. Consider a differential problem such as

$$\vartheta''(x_1,\eta)+\vartheta(x_1,\eta)+f(\vartheta)=f(x_1,\eta), \tag{11}$$

with initial conditions

$$\begin{aligned}\vartheta(x_1,0)&=a_1,\\ \vartheta_\eta(x_1,0)&=a_2,\end{aligned} \tag{12}$$

where $\vartheta(x_1,\eta)$ is a uniform function, $f(\vartheta)$ represents the nonlinear components, and $f(x_1,\eta)$ is the source term of arbitrary constants a_1 and a_2. We can also write equation (11) such as

$$\vartheta''(x_1,\eta)=-\vartheta(x_1,\eta)-f(\vartheta)+f(x_1,\eta). \tag{13}$$

In mathematics, the Sawi transform is an integral transform that converts a function of a real variable to a function of a complex variable. This transform has many applications in science and engineering because it is a tool for solving differential equations. In particular, it transforms ordinary differential equations into algebraic equations and convolution into multiplication.

Employing $\mathbb{S}T$ on equation (13), it yields

$$\mathbb{S}\left[\vartheta''(x_1,\eta)\right]=\mathbb{S}[-\vartheta(x_1,\eta)-g(\vartheta)+g(x_1,\eta)]. \tag{14}$$

Employing the propositions as defined in equation (4), we get

$$\frac{Q(\theta)}{\theta^2}-\frac{\vartheta(0)}{\theta^3}-\frac{\vartheta'(0)}{\theta^2}=-\mathbb{S}[\vartheta(x_1,\eta)+f(\vartheta)-f(x_1,\eta)]. \tag{15}$$

Thus, $Q(\theta)$ is derived as

$$Q[\theta]=\frac{\vartheta(0)}{\theta}+\vartheta'(0)-\theta^2\mathbb{S}[\vartheta(x_1,\eta)+f(\vartheta)-f(x_1,\eta)]. \tag{16}$$

Using inverse $\mathbb{S}\ T$ on equation (16), we get

$$\vartheta(x_1,\eta)=\vartheta(0)+\eta\vartheta'(0)-\mathbb{S}^{-1}\left[\theta^2\mathbb{S}\{\vartheta(x_1,\eta)+f(\vartheta)-f(x_1,\eta)\}\right], \tag{17}$$

using initial conditions, we get

$$\begin{aligned}\vartheta(x_1,\eta)=\vartheta(x_1,0)+\eta\vartheta_\eta(x_1,0)+\mathbb{S}^{-1}\left[\theta^2\mathbb{S}(f(x_1,\eta))\right]\\ -\mathbb{S}^{-1}\left[\theta^2\mathbb{S}(\vartheta(x_1,\eta)+f(\vartheta))\right].\end{aligned} \tag{18}$$

This equation (18) is the formulation of NIS of equation (11).

Now, we assume HPS such as

$$\vartheta(\eta)=\sum_{i=0}^{\infty}p^i\vartheta_i(n)=\vartheta_0+p^1\vartheta_1+p^2\vartheta_2+\cdots, \tag{19}$$

and nonlinear components $f(\vartheta)$ are defined as

$$f(\vartheta)=\sum_{i=0}^{\infty}p^iH_i(\vartheta)=H_0+p^1H_1+p^2H_2+\cdots, \tag{20}$$

we can produce the $H_n's$ as

$$H_n(\vartheta_0+\vartheta_1+\cdots+\vartheta_n)=\frac{1}{n!}\frac{\partial^n}{\partial p^n}\left(f\left(\sum_{i=0}^{\infty}p^i\vartheta_i\right)\right)_{p=0},\quad n=0,1,2,\cdots. \tag{21}$$

Using equations (19)–(21) in (18) and evaluating the similar components of p, it yields

$$\begin{aligned}&p^0\colon \vartheta_0(x_1,\eta)=G(x_1,\eta),\\ &p^1\colon \vartheta_1(x_1,\eta)=-\mathbb{S}^{-1}\left[\theta^2\mathbb{S}\{\vartheta_0(x_1,\eta)+H_0(\vartheta)\}\right],\\ &p^2\colon \vartheta_2(x_1,\eta)=-\mathbb{S}^{-1}\left[\theta^2\mathbb{S}\{\vartheta_1(x_1,\eta)+H_1(\vartheta)\}\right],\\ &p^3\colon \vartheta_3(x_1,\eta)=-\mathbb{S}^{-1}\left[\theta^2\mathbb{S}\{\vartheta_2(x_1,\eta)+H_2(\vartheta)\}\right],\\ &\vdots.\end{aligned} \tag{22}$$

On proceeding this process, which yields

$$\vartheta(x_1,\eta)=\vartheta_0+\vartheta_1+\vartheta_2+\cdots=\sum_{i=0}^{\infty}\vartheta_i. \tag{23}$$

Thus, equation (23) is a rough estimate of the differential problem's solution.

4. Numerical Applications

To demonstrate the accuracy and dependability of NIS, we offer some numerical samples. We see that, compared to earlier schemes, this method is significantly easier to implement and much simpler to generate the series of convergence. Through graphical structures, we demonstrate the physical character of the resultant plot distribution. Additionally, a graphic representation of the error distribution highlighted how close the NIS results are to the accurate solutions. We calculate the values of absolute errors by the difference of the exact solutions with the NIS results.

4.1. Example 1. Imagine a wave equation in one dimension:

$$\frac{\partial^2\vartheta}{\partial\eta^2}=\frac{\partial^2\vartheta}{\partial x_1^2}-3\vartheta, \tag{24}$$

in the initial circumstance:

$$\begin{aligned}\vartheta(x_1,0)&=0,\\ \vartheta_\eta(x_1,0)&=2\cos(x_1),\\ \vartheta(0,\eta)&=\sin(2\eta),\\ \vartheta_{x_1}(\pi,\eta)&=-\sin(2\eta).\end{aligned} \tag{25}$$

Apply $\mathbb{S}\ T$ on equation (24), we get

$$\mathbb{S}\left[\frac{\partial^2\vartheta}{\partial\eta^2}\right] = \mathbb{S}\left[\frac{\partial^2\vartheta}{\partial x_1^2} - 3\vartheta\right]. \tag{26}$$

Employing the propositions as defined in equation (4), we get

$$\frac{Q(\theta)}{\theta^2} - \frac{\vartheta(0)}{\theta^3} - \frac{\vartheta'(0)}{\theta^2} = \mathbb{S}\left[\frac{\partial^2\vartheta}{\partial x_1^2} - 3\vartheta\right]. \tag{27}$$

Thus, $Q(\theta)$ is derived as

$$Q[\theta] = \frac{\vartheta(0)}{\theta} + \vartheta'(0) + \theta^2\mathbb{S}\left[\frac{\partial^2\vartheta}{\partial x_1^2} - 3\vartheta\right]. \tag{28}$$

Using inverse $\mathbb{S}$ T, it yields

$$\vartheta(x_1,\eta) = \vartheta(x_1,0) + \eta\vartheta_\eta(x_1,0) + \mathbb{S}^{-1}\left[\theta^2\mathbb{S}\left\{\frac{\partial^2\vartheta}{\partial x_1^2} - 3\vartheta\right\}\right]. \tag{29}$$

Thus, HPS yields such as

$$\sum_{i=0}^{\infty} p^i\vartheta_i(x_1,\eta) = 2\eta\cos(x_1) + \mathbb{S}^{-1}\left[\theta^2\mathbb{S}\left\{\sum_{i=0}^{\infty} p^i\frac{\partial^2\vartheta_i}{\partial x_1^2} - 3\sum_{i=0}^{\infty} p^i\vartheta\right\}\right]. \tag{30}$$

Evaluating similar components of p, we obtain

$$\begin{aligned}
&p^0\colon \vartheta_0(x_1,\eta) = \vartheta(x_1,0) = 2\eta\cos(x_1),\\
&p^1\colon \vartheta_1(x_1,\eta) = \mathbb{S}^{-1}\left[\theta^2\mathbb{S}\left\{\frac{\partial^2\vartheta_0}{\partial x_1^2} - 3\vartheta_0\right\}\right] = -\frac{(2\eta)^3}{3!}\cos(x_1),\\
&p^2\colon \vartheta_2(x_1,\eta) = \mathbb{S}^{-1}\left[\theta^2\mathbb{S}\left\{\frac{\partial^2\vartheta_1}{\partial x_1^2} - 3\vartheta_1\right\}\right] = \frac{(2\eta)^5}{5!}\cos(x_1),\\
&p^3\colon \vartheta_3(x_1,\eta) = \mathbb{S}^{-1}\left[\theta^2\mathbb{S}\left\{\frac{\partial^2\vartheta_2}{\partial x_1^2} - 3\vartheta_2\right\}\right] = -\frac{(2\eta)^7}{7!}\cos(x_1),\\
&p^4\colon \vartheta_4(x_1,\eta) = \mathbb{S}^{-1}\left[\theta^2\mathbb{S}\left\{\frac{\partial^2\vartheta_3}{\partial x_1^2} - 3\vartheta_3\right\}\right] = \frac{(2\eta)^9}{9!}\cos(x_1),\\
&\vdots.
\end{aligned} \tag{31}$$

Similar to this, we can take into account the approximation series such that

$$\begin{aligned}
\vartheta(x_1,\eta) &= \vartheta_0(x_1,\eta) + \vartheta_1(x_1,\eta) + \vartheta_2(x_1,\eta) + \vartheta_3(x_1,\eta)\\
&\quad + \vartheta_4(x_1,\eta) + \cdots\\
&= \cos(x_1)\left(2\eta - \frac{(2\eta)^3}{3!} + \frac{(2\eta)^5}{5!} - \frac{(2\eta)^7}{7!} + \frac{(2\eta)^9}{9!}\right) + \cdots,
\end{aligned} \tag{32}$$

which can approach to

$$\vartheta(x_1,\eta) = \cos(x_1)\sin(2\eta). \tag{33}$$

Figure 1 consists of two graphs; Figure 1(a) is the NIS solution of $\vartheta(x_1,\eta)$, and Figure 1(b) is the precise solution of $\vartheta(x_1,\eta)$ at $-10 \le x_1 \le 10$ and $0 \le \eta \le 0.01$ for one-dimensional wave equation. Figure 2 demonstrates the error distribution between the obtained and the precise results at $0 \le x_1 \le 5$ along $\eta = 0.1$ and confirms the strong agreement of this scheme for problem 1. It claims that we can accurately simulate any surface to reflect the appropriate natural physical processes. Table 1 represents the absolute error between the exact solution and the NIS results. This compression shows that NIS results are very close to the exact solution and yields a fast convergence only after a few imitations.

4.2. Example 2. Imagine a wave equation in the two-dimensional form:

$$\frac{\partial^2\vartheta}{\partial\eta^2} = 2\left(\frac{\partial^2\vartheta}{\partial x_1^2} + \frac{\partial^2\vartheta}{\partial y_1^2}\right) + 6\eta + 2x_1 + 4y_1, \tag{34}$$

with the initial circumstance:

$$\begin{aligned}
\vartheta(x_1,y_1,0) &= 0,\\
\vartheta_\eta(x_1,y_1,0) &= 2\sin(x_1)\sin(y_1),\\
\vartheta(0,y_1,\eta) &= \eta^3 + 2\eta^2 y_1,\\
\vartheta_{x_1}(\pi,y_1,\eta) &= \eta^3 + \pi\eta^2 + 2\eta^2 y_1,\\
\vartheta(x_1,0,\eta) &= \eta^3 + \eta^2 x_1,\\
\vartheta_{x_1}(x_1,\pi,\eta) &= \eta^3 + 2\pi\eta^2 + \eta^2 x_1.
\end{aligned} \tag{35}$$

Apply $\mathbb{S}$ T on equation (34), we get

$$\mathbb{S}\left[\frac{\partial^2\vartheta}{\partial\eta^2}\right] = \mathbb{S}\left[2\left(\frac{\partial^2\vartheta}{\partial x_1^2} + \frac{\partial^2\vartheta}{\partial y_1^2}\right) + 6\eta + 2x_1 + 4y_1\right]. \tag{36}$$

Employing the propositions as defined in equation (4), we get

$$\begin{aligned}
&\frac{Q(\theta)}{\theta^2} - \frac{\vartheta(0)}{\theta^3} - \frac{\vartheta'(0)}{\theta^2} = \mathbb{S}\left[2\left(\frac{\partial^2\vartheta}{\partial x_1^2} + \frac{\partial^2\vartheta}{\partial y_1^2}\right) + 6\eta + 2x_1 + 4y_1\right],\\
&\frac{Q(\theta)}{\theta^2} - \frac{\vartheta(0)}{\theta^3} - \frac{\vartheta'(0)}{\theta^2} = \mathbb{S}\left[2\left(\frac{\partial^2\vartheta}{\partial x_1^2} + \frac{\partial^2\vartheta}{\partial y_1^2}\right)\right]\\
&\qquad + 6\mathbb{S}[\eta] + 2x_1\mathbb{S}[1] + 4y_1\mathbb{S}[1].
\end{aligned} \tag{37}$$

Thus, $Q(\theta)$ is derived as

$$\begin{aligned}
Q[\theta] &= 6\theta^2 + 2x_1\theta + 4y_1\theta + \frac{\vartheta(0)}{\theta} + \vartheta'(0)\\
&\quad + \theta^2\mathbb{S}\left[2\left(\frac{\partial^2\vartheta}{\partial x_1^2} + \frac{\partial^2\vartheta}{\partial y_1^2}\right]\right.\!.
\end{aligned} \tag{38}$$

Using inverse $\mathbb{S}$ T, it yields

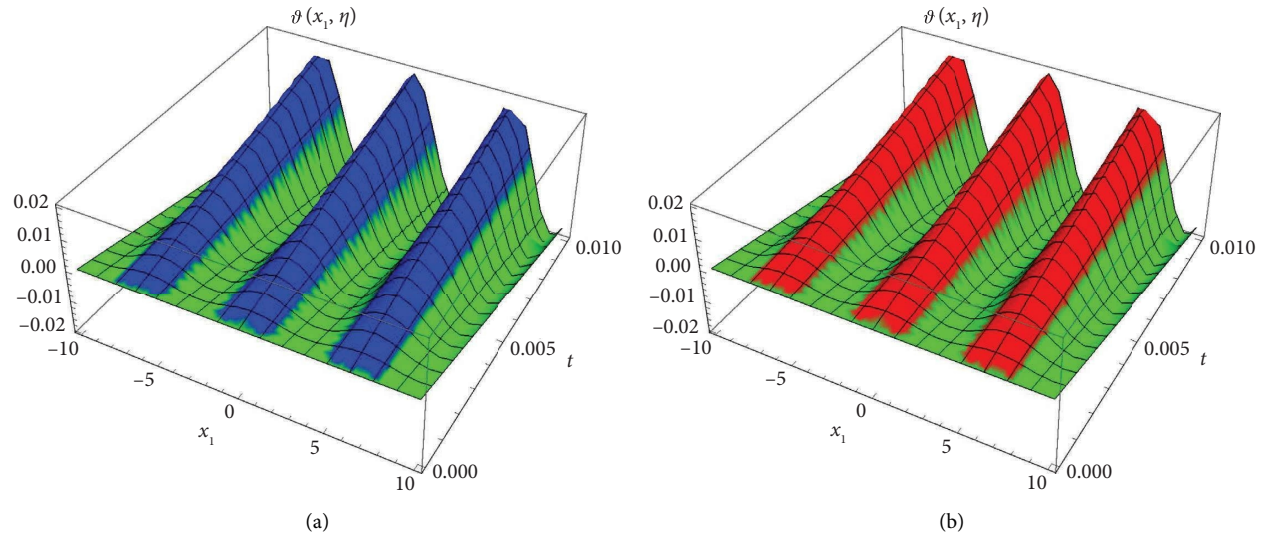

Figure 1: Surface results for one-dimensional problem. (a) 3D plot for NIS solution. (b) 3D plot for exact solution.

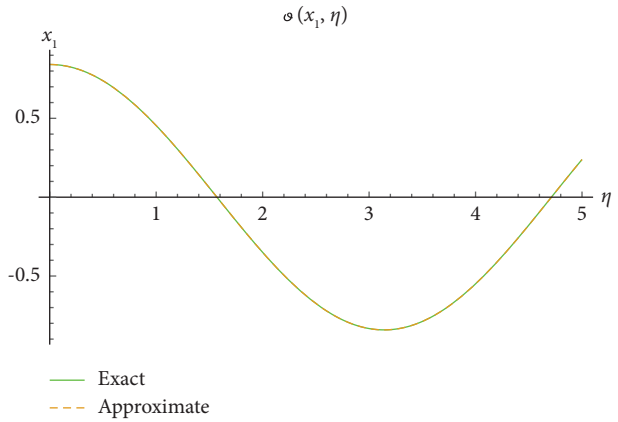

Figure 2: Error distribution among the NIS and the exact results.

Table 1: Absolute error between the NIS results and the exact results of $\vartheta(x_1, \eta)$ along x-space at various points of η for Example 1.

x_1	η	Approximate solution	Exact solution	Absolute error
0.25	0.2	0.377312	0.377312	00000
	0.4	0.695055	0.695055	00000
	0.6	0.903064	0.903064	00000
	0.8	0.968503	0.968499	4×10^{-6}
	1	0.881078	0.88103	0.000048
0.50	0.2	0.341747	0.341747	00000
	0.4	0.629539	0.629539	00000
	0.6	0.817941	0.817941	00000
	0.8	0.877212	0.877208	4×10^{-6}
	1	0.798627	0.797984	0.000043
0.75	0.2	0.284933	0.284933	00000
	0.4	0.524881	0.524881	00000
	0.6	0.681963	0.681963	00000
	0.8	0.73138	0.731377	3×10^{-6}
	1	0.665359	0.665323	0.000036
1	0.2	0.210404	0.210404	00000
	0.4	0.387589	0.387589	00000
	0.6	0.503583	0.503583	00000
	0.8	0.540074	0.540072	2×10^{-6}
	1	0.491323	0.491295	0.000028

$$\vartheta(x_1, y_1, \eta) = \eta^3 + x_1\eta^2 + 2y_1\eta^2 + \vartheta(x_1, 0) + \eta\vartheta_\eta(x_1, 0) + \mathbb{S}^{-1}\left[\theta^2\mathbb{S}\left\{2\left(\frac{\partial^2\vartheta}{\partial x_1^2} + \frac{\partial^2\vartheta}{\partial y_1^2}\right\}\right]\right]. \tag{39}$$

Thus, HPS yields such as

$$\sum_{i=0}^{\infty} p^i\vartheta_i(x_1, y_1, \eta) = \eta^3 + x_1\eta^2 + 2y_1\eta^2 + 2\eta\sin(x_1)\sin(y_1) + \mathbb{S}^{-1}\left[\theta^2\mathbb{S}\left\{2\left(\sum_{i=0}^{\infty} p^i\frac{\partial^2\vartheta_i}{\partial x_1^2} + \sum_{i=0}^{\infty} p^i\frac{\partial^2\vartheta_i}{\partial y_1^2}\right)\right\}\right]. \tag{40}$$

Comparing the same elements of p, we get

$$\begin{aligned}
p^0&: \vartheta_0(x_1, y_1, \eta) = \vartheta(x_1, 0) = \eta^3 + x_1\eta^2 + 2y_1\eta^2 + 2\eta\sin(x_1)\sin(y_1),\\
p^1&: \vartheta_1(x_1, y_1, \eta) = \mathbb{S}^{-1}\left[\theta^2\mathbb{S}\left\{\frac{\partial^2\vartheta_0}{\partial x_1^2} + \frac{\partial^2\vartheta_0}{\partial y_1^2}\right\}\right] = -\frac{(2\eta)^3}{3!}\sin(x_1)\sin(y_1),\\
p^2&: \vartheta_2(x_1, y_1, \eta) = \mathbb{S}^{-1}\left[\theta^2\mathbb{S}\left\{\frac{\partial^2\vartheta_1}{\partial x_1^2} + \frac{\partial^2\vartheta_1}{\partial y_1^2}\right\}\right] = \frac{(2\eta)^5}{5!}\sin(x_1)\sin(y_1),\\
p^3&: \vartheta_3(x_1, y_1, \eta) = \mathbb{S}^{-1}\left[\theta^2\mathbb{S}\left\{\frac{\partial^2\vartheta_2}{\partial x_1^2} + \frac{\partial^2\vartheta_2}{\partial y_1^2}\right\}\right] = -\frac{(2\eta)^7}{7!}\sin(x_1)\sin(y_1),\\
p^4&: \vartheta_4(x_1, y_1, \eta) = \mathbb{S}^{-1}\left[\theta^2\mathbb{S}\left\{\frac{\partial^2\vartheta_3}{\partial x_1^2} + \frac{\partial^2\vartheta_3}{\partial y_1^2}\right\}\right] = \frac{(2\eta)^9}{9!}\sin(x_1)\sin(y_1),\\
&\vdots .
\end{aligned} \tag{41}$$

Similar to this, we can take into account the approximation series such that

$$\begin{aligned}
\vartheta(x_1, y_1, \eta) &= \vartheta_0(x_1, y_1, \eta) + \vartheta_1(x_1, y_1, \eta) + \vartheta_2(x_1, y_1, \eta) + \vartheta_3(x_1, y_1, \eta) + \vartheta_4(x_1, y_1, \eta) + \cdots\\
&= \eta^3 + x_1\eta^2 + 2y_1\eta^2 + \sin(x_1)\sin(y_1)\cdot\left(2\eta - \frac{(2\eta)^3}{3!} + \frac{(2\eta)^5}{5!} - \frac{(2\eta)^7}{7!} + \frac{(2\eta)^9}{9!}\right) + \cdots,
\end{aligned} \tag{42}$$

which can approach to

$$\vartheta(x_1, y_1, \eta) = \eta^3 + x_1\eta^2 + 2y_1\eta^2 + \sin(x_1)\sin(y_1)\sin(2\eta). \tag{43}$$

Figure 3 consists of two graphs; Figure 3(a) is the NIS solution of $\vartheta(x_1, y_1, \eta)$, and Figure 3(b) is the precise solution of $\vartheta(x_1, y_1, \eta)$ at $-5 \le x_1 \le 5$, $0 \le \eta \le 0.01$ along $y_1 = 0.5$ for two-dimensional wave equation. Figure 4 demonstrates the error distribution between the obtained and the precise results at $0 \le x_1 \le 5$, $y_1 = 0.1$ along $\eta = 0.1$ and confirms the strong agreement of this scheme for problem 2. It claims that we can accurately simulate any surface to reflect the appropriate natural physical processes. Table 2 represents the absolute error between the exact solution and the NIS results. This compression shows that NIS results are very close to the exact solution and yields a fast convergence only after a few imitations.

4.3. Example 3. We take into consideration the three-dimensional wave problem.

$$\frac{\partial^2\vartheta}{\partial\eta^2} = \frac{x_1^2}{18}\frac{\partial^2\vartheta}{\partial x_1^2} + \frac{y_1^2}{18}\frac{\partial^2\vartheta}{\partial y_1^2} + \frac{z_1^2}{18}\frac{\partial^2\vartheta}{\partial z_1^2} - \vartheta, \tag{44}$$

with the initial condition

$$\begin{aligned}
\vartheta(x_1, y_1, z_1, 0) &= 0,\\
\vartheta_\eta(x_1, y_1, z_1, 0) &= x_1^4y_1^4z_1^4,
\end{aligned} \tag{45}$$

and boundary condition

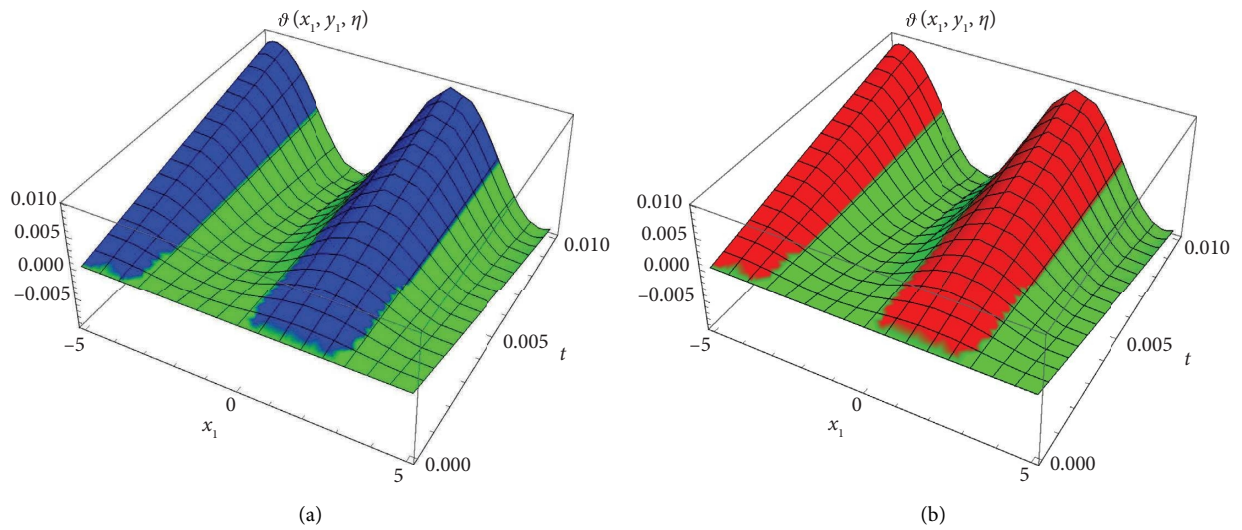

Figure 3: Surface results for two-dimensional problem. (a) 3D plot for NIS solution. (b) 3D plot for exact solution.

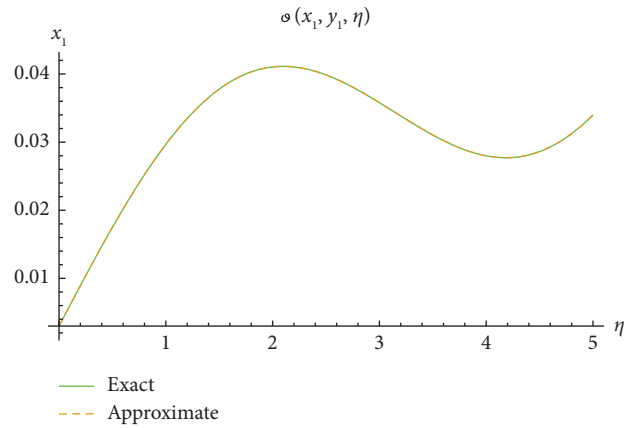

Figure 4: Error distribution among the NIS and the exact results.

Table 2: Absolute error between the NIS results and the exact results of $\vartheta(x_1, y_1, \eta)$ along x_1-space and $y_1 = 0.5$ at various points of η for Example 2.

x_1	η	Approximate solution	Exact solution	Absolute error
0.50	1	0.964469	0.964469	000000
	1.25	1.07034	1.07034	000000
	1.50	1.15241	1.15241	000000
	1.75	1.20946	1.20946	000000
	2	1.24183	1.24183	000000
1	1	3.36685	3.66683	000002
	1.25	3.66372	3.6637	000002
	1.50	3.93487	3.93481	000002
	1.75	4.17898	4.17896	000002
	2	4.39642	4.3964	000002
1.5	1	7.93362	7.93193	0.00169
	1.25	8.50361	8.50171	0.00190
	1.50	9.06949	9.06749	0.00200
	1.75	9.63105	9.62907	0.00198
	2	10.1883	10.1865	0.00180
2	1	15.733	15.6947	0.03830
	1.25	16.6989	16.6557	0.04320
	1.50	17.6835	17.6381	0.04540
	1.75	18.6878	18.643	0.04480
	2	19.7115	19.6701	0.04140

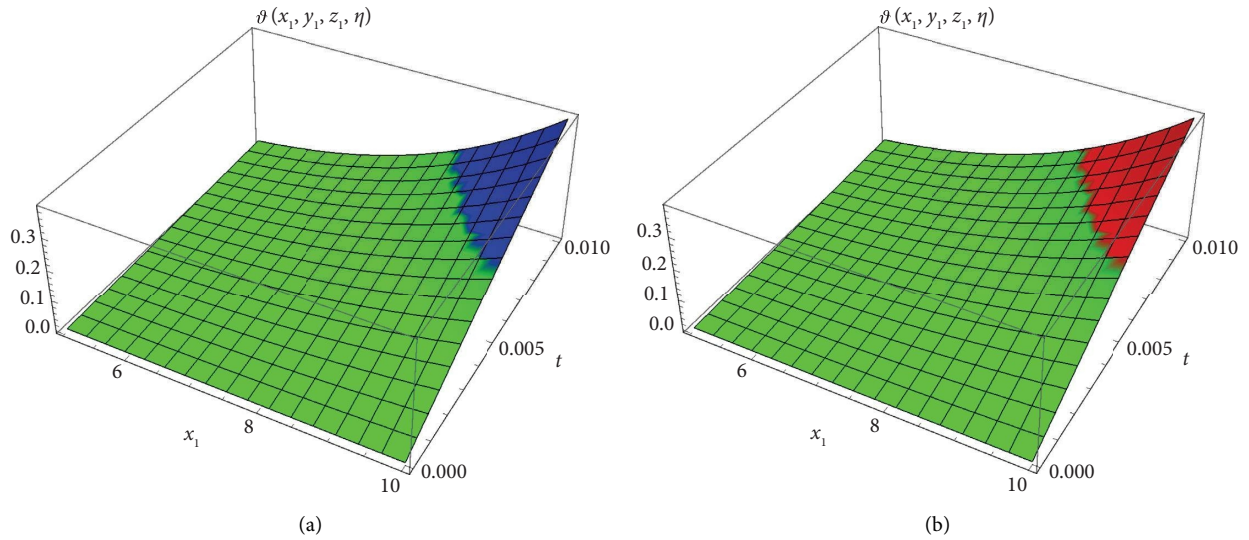

Figure 5: Surface results for three-dimensional problem. (a) 3D plot for NIS solution. (b) 3D plot for exact solution.

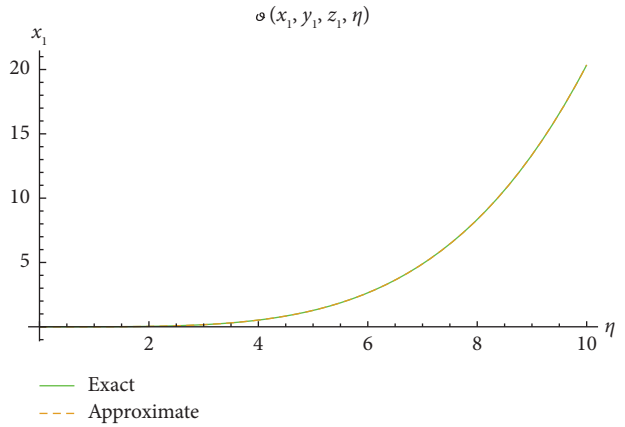

Figure 6: Error distribution among the NIS and the exact results.

Table 3: Absolute error between the NIS results and the exact results of $\vartheta(x_1, y_1, z_1, \eta)$ along x_1-space and $y_1 = z_1 = 0.5$ at various points of η for Example 3.

x_1	η	Approximate solution	Exact solution	Absolute error
0.25	1	0.0000179321	0.0000179321	00000
	1.25	0.0000244433	0.0000244433	00000
	1.50	0.0000324902	0.0000324902	00000
	1.75	0.0000425782	0.0000425783	1×10^{-10}
	2	0.0000553407	0.0000553415	8×10^{-10}
0.50	1	0.000286914	0.000286914	00000
	1.25	0.000391093	0.000391094	1×10^{-10}
	1.50	0.000519843	0.000519844	1×10^{-10}
	1.75	0.000681251	0.000681254	3×10^{-10}
	2	0.000885451	0.00088564	13×10^{-9}
0.75	1	0.0014525	0.0014525	00000
	1.25	0.00197991	0.00197991	00000
	1.50	0.00263171	0.00263171	00000
	1.75	0.00344883	0.00344885	2×10^{-18}
	2	0.0044826	0.00448266	1×10^{-7}
1	1	0.00459063	0.00459063	00000
	1.25	0.0062575	0.0062575	00000
	1.50	0.00831749	0.0083175	3×10^{-7}
	1.75	0.0109	0.0109001	1×10^{-7}
	2	0.0141672	0.0141674	2×10^{-7}

$$\begin{aligned}
&\vartheta(0, y_1, z_1, \eta) = 0,\\
&\vartheta(1, y_1, z_1, \eta) = y_1^4 z_1^4 \sinh(\eta),\\
&\vartheta(x_1, 0, z_1, \eta) = 0,\\
&\vartheta(x_1, 1, z_1, \eta) = x_1^4 z_1^4 \sinh(\eta),\\
&\vartheta(x_1, y_1, 0, \eta) = 0,\\
&\vartheta(x_1, y_1, 1, \eta) = x_1^4 y_1^4 \sinh(\eta).
\end{aligned} \tag{46}$$

Applying $\mathbb{S}\ T$ on equation (44), we get

$$\mathbb{S}\left[\frac{\partial^2 \vartheta}{\partial \eta^2}\right] = \mathbb{S}\left[\frac{x_1^2}{18}\frac{\partial^2 \vartheta}{\partial x_1^2} + \frac{y_1^2}{18}\frac{\partial^2 \vartheta}{\partial y_1^2} + \frac{z_1^2}{18}\frac{\partial^2 \vartheta}{\partial z_1^2} - \vartheta\right]. \tag{47}$$

Employing the propositions as defined in equation (4), we get

$$\frac{Q(\theta)}{\theta^2} - \frac{\vartheta(0)}{\theta^3} - \frac{\vartheta'(0)}{\theta^2} = \mathbb{S}\left[\frac{x_1^2}{18}\frac{\partial^2 \vartheta}{\partial x_1^2} + \frac{y_1^2}{18}\frac{\partial^2 \vartheta}{\partial y_1^2} + \frac{z_1^2}{18}\frac{\partial^2 \vartheta}{\partial z_1^2} - \vartheta\right]. \tag{48}$$

Thus, $Q(\theta)$ is derived as

$$Q[\theta] = \frac{\vartheta(0)}{\theta} + \vartheta'(0) + \theta^2 \mathbb{S}\left[\frac{x_1^2}{18}\frac{\partial^2 \vartheta}{\partial x_1^2} + \frac{y_1^2}{18}\frac{\partial^2 \vartheta}{\partial y_1^2} + \frac{z_1^2}{18}\frac{\partial^2 \vartheta}{\partial z_1^2} - \vartheta\right]. \tag{49}$$

Using inverse $\mathbb{S}T$, it yields

$$\begin{aligned}
\vartheta(x_1, y_1, z_1, \eta) = \vartheta(x_1, 0) + \eta \vartheta_\eta(x_1, 0)\\
+ \mathbb{S}^{-1}\left[\theta^2 \mathbb{S}\left\{\frac{x_1^2}{18}\frac{\partial^2 \vartheta}{\partial x_1^2} + \frac{y_1^2}{18}\frac{\partial^2 \vartheta}{\partial y_1^2} + \frac{z_1^2}{18}\frac{\partial^2 \vartheta}{\partial z_1^2} - \vartheta\right\}\right].
\end{aligned} \tag{50}$$

Thus, HPS yields such as

$$\sum_{i=0}^{\infty} p^i \vartheta(x_1, y_1, z_1, \eta) = \eta x_1^4 y_1^4 z_1^4 + \mathbb{S}^{-1}\left[\theta^2 \mathbb{S}\left[\sum_{i=0}^{\infty} p^i \frac{x_1^2}{18}\frac{\partial^2 \vartheta_i}{\partial x_1^2} + \sum_{i=0}^{\infty} p^i \frac{y_1^2}{18}\frac{\partial^2 \vartheta_i}{\partial y_1^2} + \sum_{i=0}^{\infty} p^i \frac{z_1^2}{18}\frac{\partial^2 \vartheta_i}{\partial z_1^2} - \sum_{i=0}^{\infty} p^i \vartheta\right]\right]. \tag{51}$$

Evaluating similar components of p, we obtain

$$\begin{aligned}
&p^0\colon \vartheta_0(x_1, y_1, z_1, \eta) = \vartheta(x_1, y_1, z_1, 0) = \eta x_1^4 y_1^4 z_1^4,\\
&p^1\colon \vartheta_1(x_1, y_1, z_1, \eta) = \mathbb{S}^{-1}\left[\theta \mathbb{S}\left\{\frac{x_1^2}{18}\frac{\partial^2 \vartheta_0}{\partial x_1^2} + \frac{y_1^2}{18}\frac{\partial^2 \vartheta_0}{\partial y_1^2} + \frac{z_1^2}{18}\frac{\partial^2 \vartheta_0}{\partial z_1^2} - \vartheta_0\right\}\right] = \frac{\eta^3}{3!} x_1^4 y_1^4 z_1^4,\\
&p^2\colon \vartheta_2(x_1, y_1, z_1, \eta) = \mathbb{S}^{-1}\left[\theta \mathbb{S}\left\{\frac{x_1^2}{18}\frac{\partial^2 \vartheta_1}{\partial x_1^2} + \frac{y_1^2}{18}\frac{\partial^2 \vartheta_1}{\partial y_1^2} + \frac{z_1^2}{18}\frac{\partial^2 \vartheta_1}{\partial z_1^2} - \vartheta_1\right\}\right] = \frac{\eta^5}{5!} x_1^4 y_1^4 z_1^4,\\
&p^3\colon \vartheta_3(x_1, y_1, z_1, \eta) = \mathbb{S}^{-1}\left[2\theta \mathbb{S}\left\{\frac{x_1^2}{18}\frac{\partial^2 \vartheta_2}{\partial x_1^2} + \frac{y_1^2}{18}\frac{\partial^2 \vartheta_2}{\partial y_1^2} + \frac{z_1^2}{18}\frac{\partial^2 \vartheta_2}{\partial z_1^2} - \vartheta_2\right\}\right] = \frac{\eta^7}{7!} x_1^4 y_1^4 z_1^4,\\
&p^4\colon \vartheta_4(x_1, y_1, z_1, \eta) = \mathbb{S}^{-1}\left[\theta \mathbb{S}\left\{\frac{x_1^2}{18}\frac{\partial^2 \vartheta_3}{\partial x_1^2} + \frac{y_1^2}{18}\frac{\partial^2 \vartheta_3}{\partial y_1^2} + \frac{z_1^2}{18}\frac{\partial^2 \vartheta_3}{\partial z_1^2} - \vartheta_3\right\}\right] = \frac{\eta^9}{9!} x_1^4 y_1^4 z_1^4,\\
&\vdots .
\end{aligned} \tag{52}$$

Similar to this, we can take into account the approximation series such that

$$\begin{aligned}
\vartheta(x_1, y_1, z_1, \eta) &= \vartheta_0(x_1, y_1, z_1, \eta) + \vartheta_1(x_1, y_1, z_1, \eta) + \vartheta_2(x_1, y_1, z_1, \eta) + \vartheta_3(x_1, y_1, z_1, \eta) + \vartheta_4(x_1, y_1, z_1, \eta) + \cdots\\
&= x_1^4 y_1^4 z_1^4 \left(\eta + \frac{\eta^3}{3!} + \frac{\eta^5}{5!} + \frac{\eta^7}{7!} + \frac{\eta^9}{9!}\right) + \cdots,
\end{aligned} \tag{53}$$

which can approach to

$$\vartheta(x_1, y_1, z_1, \eta) = x_1^4 y_1^4 z_1^4 \sinh(\eta). \tag{54}$$

Figure 5 consists of two graphs; Figure 5(a) is the NIS solution of $\vartheta(x_1, y_1, z_1, \eta)$, and Figure 5(b) is the precise solution of $\vartheta(x_1, y_1, z_1, \eta)$ at $5 \le x_1 \le 10$ and $0 \le \eta \le 0.01$ with $y_1 = 0.5$ and $z_1 = 0.5$ for three-dimensional wave equation. Figure 6 demonstrates the error distribution between the obtained and the precise results at $0 \le x_1 \le 10$, $y_1 = 0.5$, $y_1 = 0.5$ along $\eta = 0.5$ and confirms the strong agreement of this scheme for problem 3. It claims that we can accurately simulate any surface to reflect the appropriate natural physical processes. Table 3 represents the absolute error between the exact solution and the NIS results. This compression shows that NIS results are very close to the exact solution and yields a fast convergence only after a few imitations.

5. Conclusion and Future Work

This article presents the study of a new iterative scheme (NIS) using the combination of Sawi integral transform and HPS for the approximate results of multidimensional wave problems. This NIS derives the results with the consistency of analysis from the recurrence relation. The derived results from numerical examples demonstrate that our scheme is very easy to implement and the rate of convergence is higher than other approaches. The 3D graphical representations show the physical behavior of the problems, and 2D plots' distribution represents the visual error among the obtained and the precise results. We show that NIS has the best agreement with the precise solutions to the problems. We aim to apply this scheme the nonlinear and fractional differential problems in our future work.

Data Availability

The data used to support the findings of this study are available on request from the corresponding author.

Conflicts of Interest

The authors declare that they have no conflicts of interest.

References

[1] W. A. Khan, "Numerical simulation of chun-hui he's iteration method with applications in engineering," *International Journal of Numerical Methods for Heat and Fluid Flow*, vol. 32, no. 3, pp. 944–955, 2021.

[2] K. A. Gepreel and A. Al-Thobaiti, "Exact solutions of nonlinear partial fractional differential equations using fractional sub-equation method," *Indian Journal of Physics*, vol. 88, no. 3, pp. 293–300, 2014.

[3] A. Althobaiti, S. Althobaiti, K. El-Rashidy, and A. R. Seadawy, "Exact solutions for the nonlinear extended kdv equation in a stratified shear flow using modified exponential rational method," *Results in Physics*, vol. 29, Article ID 104723, 2021.

[4] T. Gul, A. Qadeer, W. Alghamdi, A. Saeed, S. Mukhtar, and M. Jawad, "Irreversibility analysis of the couple stress hybrid nanofluid flow under the effect of electromagnetic field," *International Journal of Numerical Methods for Heat and Fluid Flow*, vol. 32, no. 2, pp. 642–659, 2021.

[5] M. Cakmak and S. Alkan, "A numerical method for solving a class of systems of nonlinear pantograph differential equations," *Alexandria Engineering Journal*, vol. 61, no. 4, pp. 2651–2661, 2022.

[6] S. Momani and Z. Odibat, "Analytical approach to linear fractional partial differential equations arising in fluid mechanics," *Physics Letters A*, vol. 355, no. 4-5, pp. 271–279, 2006.

[7] M. Dehghan, J. Manafian, and A. Saadatmandi, "Key words: nonlinear differential-difference equations; exp-function method; N-soliton solutions," *Zeitschrift für Naturforschung A*, vol. 65, no. 11, pp. 935–949, 2010.

[8] K. Raslan, K. K. Ali, and M. A. Shallal, "The modified extended tanh method with the Riccati equation for solving the space-time fractional EW and MEW equations," *Chaos, Solitons and Fractals*, vol. 103, pp. 404–409, 2017.

[9] H. Rezazadeh, N. Ullah, L. Akinyemi et al., "Optical soliton solutions of the generalized non-autonomous nonlinear Schrödinger equations by the new kudryashov's method," *Results in Physics*, vol. 24, Article ID 104179, 2021.

[10] J. Biazar and H. Ghazvini, "Convergence of the homotopy perturbation method for partial differential equations," *Nonlinear Analysis: Real World Applications*, vol. 10, no. 5, pp. 2633–2640, 2009.

[11] S. T. Mohyud-Din and M. A. Noor, "Homotopy perturbation method for solving partial differential equations," *Zeitschrift für Naturforschung A*, vol. 64, no. 3-4, pp. 157–170, 2009.

[12] J.-H. He, Y. O. El-Dib, and A. A. Mady, "Homotopy perturbation method for the fractal toda oscillator," *Fractal and Fractional*, vol. 5, no. 3, p. 93, 2021.

[13] M. Nadeem, J.-H. He, and A. Islam, "The homotopy perturbation method for fractional differential equations: part 1 mohand transform," *International Journal of Numerical Methods for Heat and Fluid Flow*, vol. 31, no. 11, pp. 3490–3504, 2021.

[14] A.-M. Wazwaz, "The variational iteration method: a reliable analytic tool for solving linear and nonlinear wave equations," *Computers and Mathematics with Applications*, vol. 54, no. 7-8, pp. 926–932, 2007.

[15] M. Ghasemi, M. Tavassoli Kajani, and A. Davari, "Numerical solution of two-dimensional nonlinear differential equation by homotopy perturbation method," *Applied Mathematics and Computation*, vol. 189, no. 1, pp. 341–345, 2007.

[16] Y. Keskin and G. Oturanc, "Reduced differential transform method for solving linear and nonlinear wave equations," *Iranian Journal of Science and Technology Transaction A-Science*, vol. 34, no. 2, pp. 133–142, 2010.

[17] H. Ullah, S. Islam, L. Dennis, T. Abdelhameed, I. Khan, and M. Fiza, "Approximate solution of two-dimensional nonlinear wave equation by optimal homotopy asymptotic method," *Mathematical Problems in Engineering*, vol. 2015, Article ID 380104, 7 pages, 2015.

[18] M. Adwan, M. Al-Jawary, J. Tibaut, and J. Ravnik, "Analytic and numerical solutions for linear and nonlinear multidimensional wave equations," *Arab Journal of Basic and Applied Sciences*, vol. 27, no. 1, pp. 166–182, 2020.

[19] M. Jleli, S. Kumar, R. Kumar, and B. Samet, "Analytical approach for time fractional wave equations in the sense of yang-abdel-aty-cattani via the homotopy perturbation transform method," *Alexandria Engineering Journal*, vol. 59, no. 5, pp. 2859–2863, 2020.

[20] R. Mullen and T. Belytschko, "Dispersion analysis of finite element semidiscretizations of the two-dimensional wave equation," *International Journal for Numerical Methods in Engineering*, vol. 18, no. 1, pp. 11–29, 1982.
[21] G. P. Singh and S. Aggarwal, "Sawi transform for population growth and decay problems," *International Journal of Latest Technology in Engineering, Management and Applied Science*, vol. 8, no. 8, pp. 157–162, 2019.
[22] M. Higazy, S. Aggarwal, and T. A. Nofal, "Sawi decomposition method for volterra integral equation with application," *Journal of Mathematics*, vol. 2020, Article ID 6687134, 13 pages, 2020.
[23] M. M. A. Mahgoub, "The new integral transform sawi transform," *Advances in Theoretical and Applied Mathematics*, vol. 14, no. 1, pp. 81–87, 2019.
[24] M. Higazy and S. Aggarwal, "Sawi transformation for system of ordinary differential equations with application," *Ain Shams Engineering Journal*, vol. 12, no. 3, pp. 3173–3182, 2021.
[25] H. Jafari, "A new general integral transform for solving integral equations," *Journal of Advanced Research*, vol. 32, pp. 133–138, 2021.